

US EPA ARCHIVE DOCUMENT

**EXAMINATION OF METALS TRANSPORT UNDER  
HIGHLY ALKALINE CONDITIONS**

Contract No. 68-C6-0020  
WORK ASSIGNMENT NO. 0-07

June 19, 1997

## Table of Contents

List of Tables .....	iii
List of Figures .....	iv
1.0 INTRODUCTION .....	1
2.0 DETERMINATION OF $K_d$ VALUES FOR CKD DISPOSAL .....	2
3.0 RESULTS .....	7
4.0 COMPARISON WITH HWIR RESULTS .....	18
5.0 CONCLUSIONS .....	24
6.0 REFERENCES .....	24
Appendix A .....	25
Appendix B .....	27
Appendix C .....	30



## List of Tables

Table 2.1. Contribution of CKD inorganic leachate constituents . . . . .	3
Table 2.2. MINTEQA2 constituent concentrations in CKD modeling . . . . .	4
Table 2.3. Other MINTEQA2 program settings and options. . . . .	5



## List of Figures

Figure 3.1. Log $K_d$ (L/kg) vs. log total Pb (mg/L) at pH 11, 12, and 13 in the unsaturated zone. . . . .	8
Figure 3.2. Log $K_d$ (L/kg) vs. log total Pb (mg/L) at pH 11, 12, and 13 in the saturated zone. . . . .	9
Figure 3.3. Log $K_d$ (L/kg) vs. log total Cd (mg/L) at pH 11, 12, and 13 in the unsaturated zone. . . . .	10
Figure 3.4. Log $K_d$ (L/kg) vs. log total Cd (mg/L) at pH 11, 12, and 13 in the saturated zone. . . . .	11
Figure 3.5. Log $K_d$ (L/kg) vs. log total Cr(III) (mg/L) at pH 11, 12, and 13 in the unsaturated zone. . . . .	12
Figure 3.6. Log $K_d$ (L/kg) vs. log total Cr(III) (mg/L) at pH 11, 12, and 13 in the saturated zone. . . . .	13
Figure 3.7. Log $K_d$ (L/kg) vs. log total Ba (mg/L) at pH 11, 12, and 13 in the unsaturated zone. . . . .	14
Figure 3.8. Log $K_d$ (L/kg) vs. log total Ba (mg/L) at pH 11, 12, and 13 in the saturated zone. . . . .	15
Figure 3.9. Log $K_d$ (L/kg) vs. log total Be (mg/L) at pH 11, 12, and 13 in the unsaturated zone. . . . .	16
Figure 3.10. Log $K_d$ (L/kg) vs. log total Be (mg/L) at pH 11, 12, and 13 in the saturated zone. . . . .	17
Figure 4.1. HWIR results: log $K_d$ (L/kg) vs. log total Pb (mg/L) at pH 8 in the unsaturated and saturated zones. . . . .	20
Figure 4.2. HWIR results: log $K_d$ (L/kg) vs. log total Cd (mg/L) at pH 8 the unsaturated and saturated zones. . . . .	21
Figure 4.3. HWIR results: log $K_d$ (L/kg) vs. log total Cr(III) (mg/L) at pH 8 in the unsaturated and saturated zones. . . . .	22
Figure 4.4. HWIR results: log $K_d$ (L/kg) vs. log total Ba (mg/L) at pH 8 in the unsaturated and saturated zones. . . . .	23

## 1.0 INTRODUCTION

This report presents metal adsorption distribution coefficients ( $K_d$  values) for the metals barium (Ba), beryllium (Be), cadmium (Cd), chromium(III) (Cr(III)), and lead (Pb) in groundwater under the highly alkaline conditions possible with land disposal of cement kiln dust (CKD).  $K_d$  is the ratio of concentration sorbed to concentration in the dissolved phase at equilibrium. The  $K_d$  values were determined using the U.S. EPA geochemical speciation model, MINTEQA2. The abovementioned metals along with antimony, arsenic, chromium(VI), and thallium were the subject of an earlier metal transport study employing  $K_d$  values from the Hazardous Waste Identification Rule (HWIR). The purpose of the current study is to assess whether the  $K_d$  values from HWIR can be used in the highly alkaline conditions expected from CKD disposal. Earlier in this study, an assessment of the applicability of HWIR  $K_d$  values to the CKD disposal scenario identified Ba, Be, Cd, Cr(III), and Pb as the metals most likely to have adsorptive behavior significantly different from the HWIR Subtitle D landfill scenario. The  $K_d$  values for the metals presented in this report are the result of modifying the HWIR modeling parameters to reflect groundwater conditions expected in land disposal of CKD.

The HWIR  $K_d$  values are represented as functions of several variables including metal concentration, concentration of leachate organic acids, concentration of natural organic matter (particulate (POM) and dissolved (DOM)), concentration of hydrous ferric oxide (HFO) sorbent, and pH. Hydrous ferric oxide is the primary sorbing phase with additional sorption onto POM. One primary difference in HWIR and CKD modeling scenarios is the pH. Specifically, the highest pH considered in HWIR modeling was 8.0. For CKD disposal, pH may range as high as 13. This report presents new  $K_d$  values at pH 11.0, 12.0, and 13.0.

Another significant difference in HWIR and CKD scenarios is related to leachate quality. The HWIR modeling for  $K_d$  values assumed the presence of anthropogenic organic acids in the leachate from the decomposition of municipal and industrial wastes. Accordingly, three representative organic acids were included in the HWIR speciation modeling (MINTEQA2). The disposal of CKD envisioned here is via a monofill in which the anthropogenic organic acid component would not be significant. However, there could be elevated concentrations of certain inorganic constituents from CKD leaching. In this study, no data was available on the concentrations of major ions in CKD leachate. Therefore, the MINTEQA2 model was used in preliminary modeling to simulate the Toxicity Characteristic Leaching Procedure (TCLP) on CKD. The purpose of this simulation was to estimate the concentrations of major inorganic ions in CKD leachate so that these could be included in subsequent MINTEQA2 modeling for  $K_d$  values.

The previous groundwater transport modeling for the CKD scenario employed the HWIR  $K_d$  values corresponding to the medium concentration settings of HFO and POM. Therefore, only the medium settings of HFO and POM were used in the determination of the  $K_d$  values presented here.

## 2.0 DETERMINATION OF $K_d$ VALUES FOR CKD DISPOSAL

The  $K_d$  values were calculated using the U.S. EPA geochemical speciation model MINTEQA2<sup>1</sup> with model parameters consistent with those used to derive  $K_d$  values for the groundwater pathway in the Hazardous Waste Identification Rule (HWIR) (USEPA, 1996). The modeling scenario for HWIR was developed to represent Subtitle D landfill disposal. That scenario has been modified here to represent the highly alkaline conditions possible beneath a land disposal unit for cement kiln dust (CKD). As for the HWIR modeling, the CKD  $K_d$  values have been modeled separately for the unsaturated and saturated zones. Also, consistent with HWIR modeling, the  $K_d$  values reported here were determined as a function of total metal concentration.

The modeling was preceded by a database update for relevant metals and CKD ligands employing the *NIST Critical Stability Constants, Reference Database 46, version 2.0*. Equilibrium constants from the NIST database were corrected to zero ionic strength if needed (as required for use in MINTEQA2). NIST reactions were re-formulated in terms of MINTEQA2 components. In addition, the database of HFO-metal adsorption reactions was updated with data from Dzombak and Morel, 1990. The most significant change in the database was the addition of solution, HFO-sorption, and precipitation reactions for beryllium. Appendix A presents a listing of reactions added or updated in the course of this study.

### 2.1 Modifications of the HWIR Modeling Parameters for CKD Disposal

Geochemical factors of primary importance included in HWIR modeling and known to have direct impact on adsorption in groundwater systems were: (1) subsurface pH, (2) hydrous ferric oxide adsorbent content of the soil/aquifer in the subsurface, (3) natural soil organic matter content of the soil/aquifer in the subsurface (particulate and dissolved), and (4) concentration of organic acids in the leachate. For a given metal at a given total concentration, the propensity for adsorption changes greatly as these parameters vary. For the HWIR modeling, the natural variability of these parameters was divided into three ranges: high, medium, and low. The only chemical characteristic of the leachate included in the HWIR modeling was the concentration of leachate organic acids. As previously mentioned, organic leachate acids are not included in CKD, and the medium concentrations only for HFO and POM were considered.

The highest pH used in the HWIR modeling was 8.0. This value represents the 92.5 percentile value from a distribution of 24,921 field measured groundwater pH values. Because CKD leachate is highly alkaline with leachate pH as high as 13, the pH range covered by HWIR modeling may not be high enough. In the HWIR modeling, it was assumed that the groundwater/aquifer system is well buffered with respect to pH. That is, in the modeling there is

---

<sup>1</sup>The MINTEQA2 model used to develop the  $K_d$  values for this work is a revision of MINTEQA2, version 3.11 (v3.11) currently being distributed by the U.S. EPA. It differs from v3.11 in several respects which are fully documented in the background document for the HWIR modeling (USEPA, 1996).

no effect on the ambient pH from the landfill leachate. This simplifying assumption may have less validity for the CKD scenario because of the highly alkaline nature of CKD leachate. An assessment of the impact of CKD leachate on ambient groundwater pH is beyond the scope of this study. As an initial step towards such an assessment, this study presents the impact on metal adsorption ( $K_d$ ) if groundwater pH is elevated to the range of 11 to 13. Specifically, three pH's are used: 11, 12, and 13. There is no statistical significance to this choice of pH values.

The concentrations of major ions in the leachate and groundwater were considered to be of secondary importance in their effect on metal adsorption in the HWIR scenario. However, for the CKD scenario, the concentrations of certain inorganic ions (Ca, Na, K, Cl, and  $SO_4$ ) that either: (i) complex the metals of interest, or (ii) compete with the metals for adsorption sites, or (iii) significantly impact the ionic strength may have a significant impact on metal adsorption. This potential for impacting metal adsorption should rightfully elevate such ions to the status of primary or *master variables* (to use the HWIR terminology). However, to be consistent with HWIR, such a status would imply that statistically meaningful concentration levels can be assigned. Unfortunately, this is not the case. Instead, for the purposes of this study, the concentrations of these five constituents will be set at the levels determined by the TCLP test on CKD. Because no measured TCLP data was available to characterize these ions, the MINTEQA2 model was used in a preliminary run (not involving adsorption) to simulate the TCLP on a CKD material having an average mineralogical composition determined from data given in Haynes and Kramer (1982). Details of how this composition was determined and the use of MINTEQA2 in simulating the TCLP are given in Appendix B.

The concentration levels of the ions in CKD leachate as determined by the TCLP simulation are shown in Table 2.1. The Table 2.1 concentrations were added to the ambient groundwater concentrations of these ions for unsaturated and saturated zone modeling. The saturated zone values are just the unsaturated zone contributions divided by seven to account for dilution due to dispersion and diffusion in the mixing zone. (This is the same dilution factor used for leachate organic acids in HWIR modeling).

Table 2.1. Contribution of CKD inorganic leachate constituents.

CKD Leachate Constituent	Unsaturated Zone Contribution (mg/L)	Saturated Zone Contribution (mg/L)
Calcium	2835	405
Sodium	300	43
Potassium	408	58
Chloride	379	54
Sulfate	632	90



A listing of all constituent concentrations used in the modeling is shown in Table 2.2. Table 2.3 shows the settings of various other parameters relevant to the MINTEQA2 modeling.

Table 2.2. MINTEQA2 constituent concentrations in CKD modeling. The concentrations of the CKD leachate constituents (Ca, Na, K, Cl, and SO<sub>4</sub>) are the sum of Table 2.1 contributions and ambient groundwater contributions from HWIR modeling.

Constituent	Concentration (mg/L <i>except as indicated</i> )	MINTEQA2 component
Aluminum	0.20	Al <sup>3+</sup>
Calcium		Ca <sup>2+</sup>
<i>Unsaturated</i>	2883.0	
<i>Saturated</i>	453.0	
Iron (III)	0.20	Fe <sup>3+</sup>
Magnesium	14.00	Mg <sup>2+</sup>
Manganese (II)	0.04	Mn <sup>2+</sup>
Potassium		K <sup>+</sup>
<i>Unsaturated</i>	410.9	
<i>Saturated</i>	60.9	
Sodium		Na <sup>+</sup>
<i>Unsaturated</i>	322.0	
<i>Saturated</i>	65.0	
Carbonate	187.00	CO <sub>3</sub> <sup>2-</sup>
Bromine	0.30	Br <sup>-</sup>
Chloride		Cl <sup>-</sup>
<i>Unsaturated</i>	394.0	
<i>Saturated</i>	69.0	
Nitrate	1.00	NO <sub>3</sub> <sup>-</sup>
Phosphate	0.09	PO <sub>4</sub> <sup>3-</sup>
Sulfate		SO <sub>4</sub> <sup>2-</sup>
<i>Unsaturated</i>	657.0	
<i>Saturated</i>	115.0	
DOM		DOM
<i>Unsaturated</i>	2.439x10 <sup>-5</sup> mol/L	
<i>Saturated</i>	1.728x10 <sup>-5</sup> mol/L	

Constituent		Concentration (mg/L <i>except as indicated</i> )	MINTEQA2 component
POM	<i>Unsaturated</i>	5.758x10 <sup>-3</sup> mol/L	POM
	<i>Saturated</i>	3.161x10 <sup>-3</sup> mol/L	
HFO, Site 1	<i>Unsaturated</i>	8.568x10 <sup>-4</sup> mol/L	SOH1
	<i>Saturated</i>	6.674x10 <sup>-4</sup> mol/L	
HFO, Site 2	<i>Unsaturated</i>	3.427x10 <sup>-2</sup> mol/L	SOH2
	<i>Saturated</i>	2.670x10 <sup>-2</sup> mol/L	

Table 2.3. Other MINTEQA2 program settings and options.

Parameter or Option	Setting	Comment
Temperature	14	°C; this is an average for U.S. groundwater obtained from the U.S. EPA STORET database
Units of concentration	mg/L	HFO, DOM, and POM in mol sites liter <sup>-1</sup>
Ionic strength (I.S.) option	I.S. to be computed	
Solids option	Solids allowed	Print equilibrium results after all solids have precipitated
Iterations (maximum)	200	
Activity coefficient equation	Davies	
Output completeness option	Full output	
Sweep option	On	48 points individually specified
Sweep parameter	Total concentration	Of contaminant metal
Auxiliary importable output option	On	Output equilibrated distribution of metal dissolved, sorbed, and precipitated
Diffuse-layer adsorption	On	One HFO surface with two site types; Attach HFO database (FEO-DLM.DBS) to input file
Specific surface area (HFO)	600.0 m <sup>2</sup> g <sup>-1</sup>	

Parameter or Option	Setting	Comment
User imposed equilibrium constraints	1	pH is specified as per above description
User imposed excluded species	2	Species number 2003002 (Diaspore) and number 3028100 (Hematite) excluded
Alkalinity	Not specified	Inorganic carbon specified as total dissolved carbonate (component 140)
Charge balance option	Off	Do not terminate due to charge imbalance

An example MINTEQA2 input file for the generation of  $K_d$ 's for Pb is shown in Appendix C. This example corresponds to the unsaturated zone modeling at pH 11.0. The set of total input concentrations for Pb shown in the example file was the same for all metals throughout the modeling. Specifically, the speciation problem was solved at a series of 48 total metal concentrations beginning with 0.001 mg liter<sup>-1</sup> and ending with 100,000 mg liter<sup>-1</sup>.

In addition to the parameters mentioned above, an inert ion of positive or negative charge was added to provide a charge balanced solution at equilibrium. MINTEQA2 does not use the charge balance equation to solve the equilibrium problem. However, charge balance in the aqueous phase will prevail in the real system, and concentrations of charged species impact the solution ionic strength. Ionic strength in turn effects activity coefficients which are used to adjust reaction equilibrium constants. The equilibrium composition including amount of metal sorbed is thus impacted by charge balance.

In summary, the modeling parameters used for the CKD scenario are the same as the HWIR modeling with the following exceptions:

- pH values of 11.0, 12.0, and 13.0 were used
- Simulated CKD leachate concentrations of Ca, Na, K, Cl, and SO<sub>4</sub> were added to the ambient HWIR concentrations for these constituents in the unsaturated zone and were diluted by a factor of seven and added to groundwater concentrations for the saturated zone
- No leachate organic acids were included
- Only the medium concentration settings for HFO and natural organic matter were used

- The thermodynamic database of reactions including the HFO-metal sorption reactions were updated. (See Appendix A.)
- In inert ion was added to provide charge balance at equilibrium.

The first two differences listed are the most significant in terms of effect on computed  $K_d$ .

### 3.0 RESULTS

Input files using the above parameters were developed for each of the five metals (Ba, Be, Cd, Cr(III), and Pb) at three pH's (11, 12, and 13) in both the unsaturated and saturated zones for a total of 30 input files. Each file was designed to solve the equilibrium composition at each of the 48 total metal concentrations. For each total metal concentration, the  $K_d$  is obtained by dividing the total sorbed by the total dissolved. The resulting dimensionless  $K_d$  is normalized by the phase ratio (the mass of adsorbing soil/aquifer material with which one liter of solution is equilibrated). In keeping with the HWIR modeling scenario, the phase ratio in the unsaturated zone was 4.57 kg per liter of solution. The phase ratio in the saturated zone was 3.56 kg per liter of solution. These values were determined for HWIR by assuming an average density and porosity of aquifer material and assuming a water saturation of 77% in unsaturated zone and 100% in the saturated zone.

A special output option in MINTEQA2 allows the total dissolved, total sorbed, and total precipitated metal concentration at equilibrium to be written to a file (with filename extension PRN) suitable for import to a spreadsheet. This facilitates calculation of  $K_d$  from the MINTEQA2 results. The PRN file also serves as an input file for using the MINTEQA2  $K_d$  values in transport modeling. There were 30 PRN files generated; six files for each of the five metals (3 pH's in the unsaturated zone, 3 in the saturated zone for each metal). Each contains 48 lines in ASCII format. Each of the 48 lines represents an equilibration point for a specific metal concentration. For consistency and ease of identification, the naming convention aaMMbbccPRN was used where "aa" is the two-letter designator of the metal (e.g., Pb, Cd, etc.), "bb" is the pH (11, 12, or 13), and "cc" is a two-letter designator of the zone (ux = unsaturated, sx = saturated). The "MM" appears in all names as an indicator that the results pertain to the medium concentration setting for HFO and organic matter. As an example, PbMM11uxPRN is the output file for Pb at pH 11 in the unsaturated zone. This file contains 48 lines, each representing an equilibration at a specific metal concentration. Each line has eight entries as follows: pH, three-digit ID # for Pb, total dissolved Pb concentration (mol/L), total sorbed Pb concentration (mol/L), total precipitated Pb concentration (mol/L), the normalized  $K_d$  (L/kg), an experimental quantity (irrelevant in this study), and the total Pb concentration (mg/L).

Graphical results obtained by plotting the log  $K_d$  versus the log total metal concentration for each of the 30 PRN files is shown on the following pages. Results at each of the 3 pH values are shown together on one page for each metal.

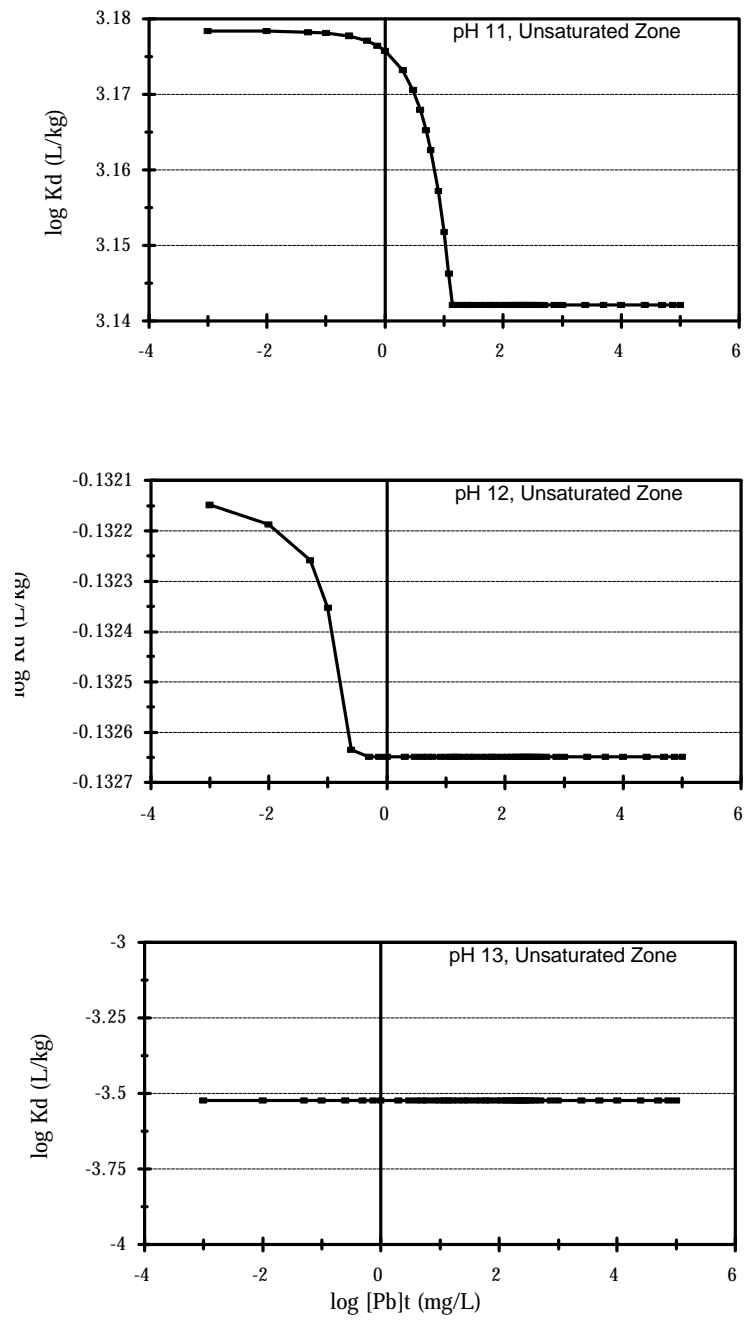


Figure 3.1. Log  $K_d$  (L/kg) vs. log total Pb (mg/L) at pH 11, 12, and 13 in the unsaturated zone.

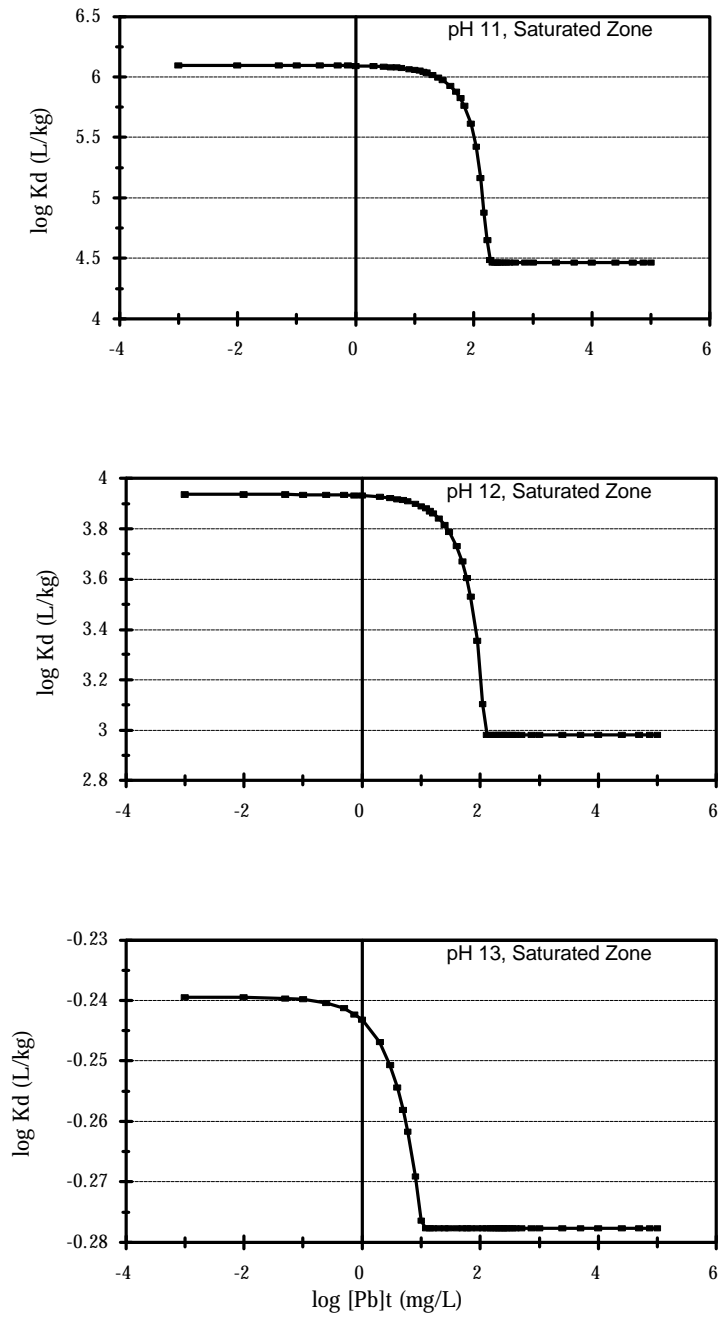


Figure 3.2.  $\log K_d$  (L/kg) vs.  $\log$  total Pb (mg/L) at pH 11, 12, and 13 in the saturated zone.

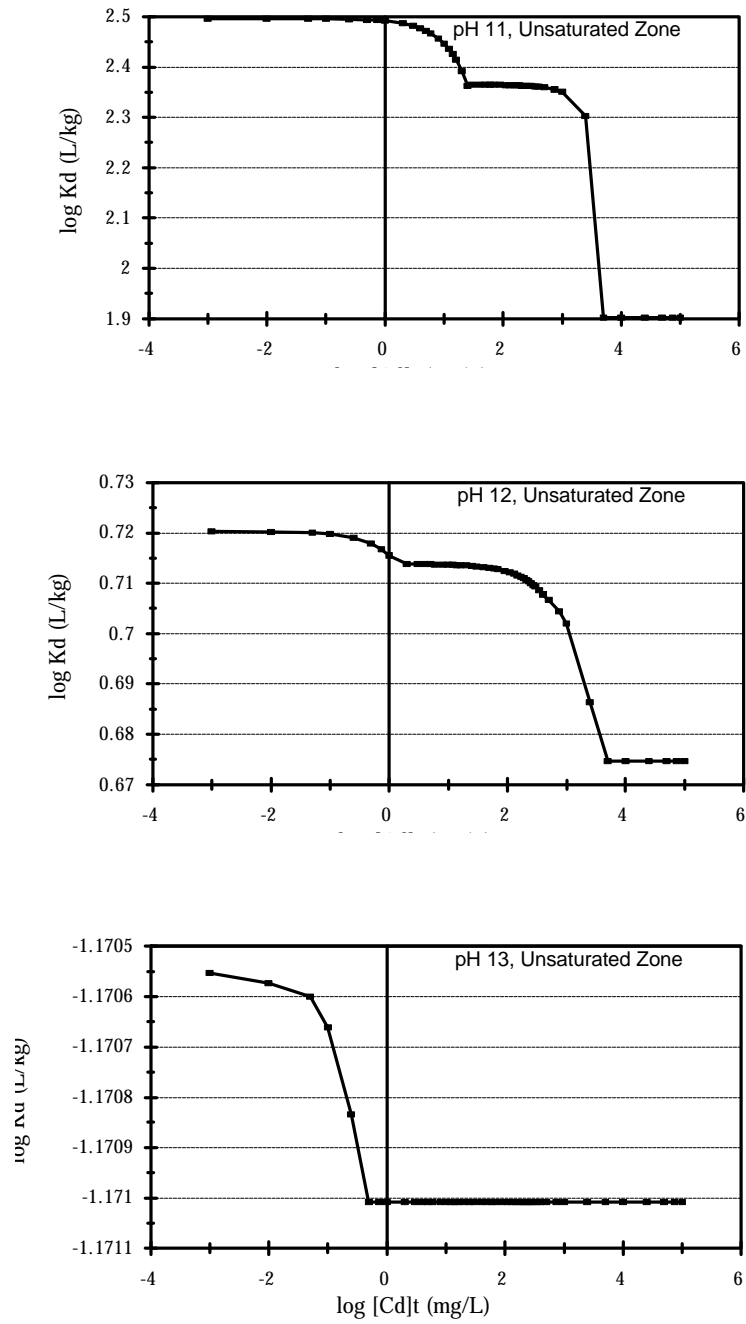


Figure 3.3. Log  $K_d$  (L/kg) vs. log total Cd (mg/L) at pH 11, 12, and 13 in the unsaturated zone.

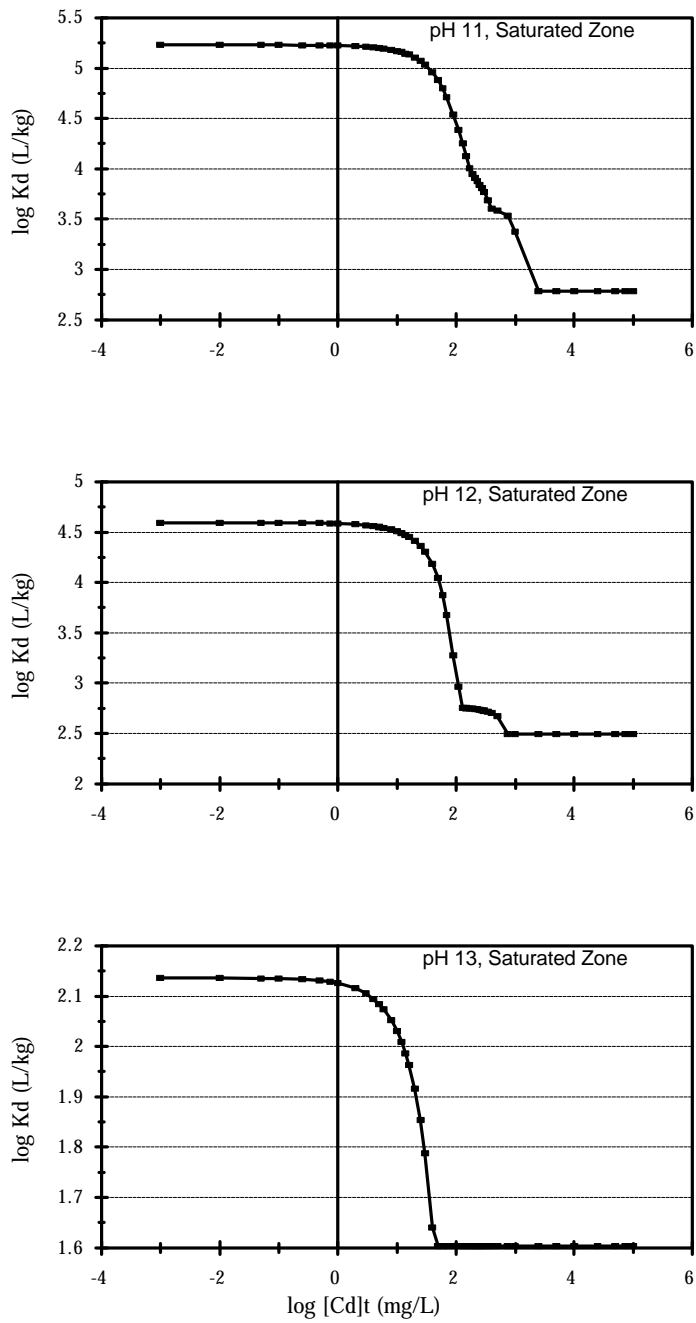


Figure 3.4.  $\log K_d$  (L/kg) vs.  $\log$  total Cd (mg/L) at pH 11, 12, and 13 in the saturated zone.



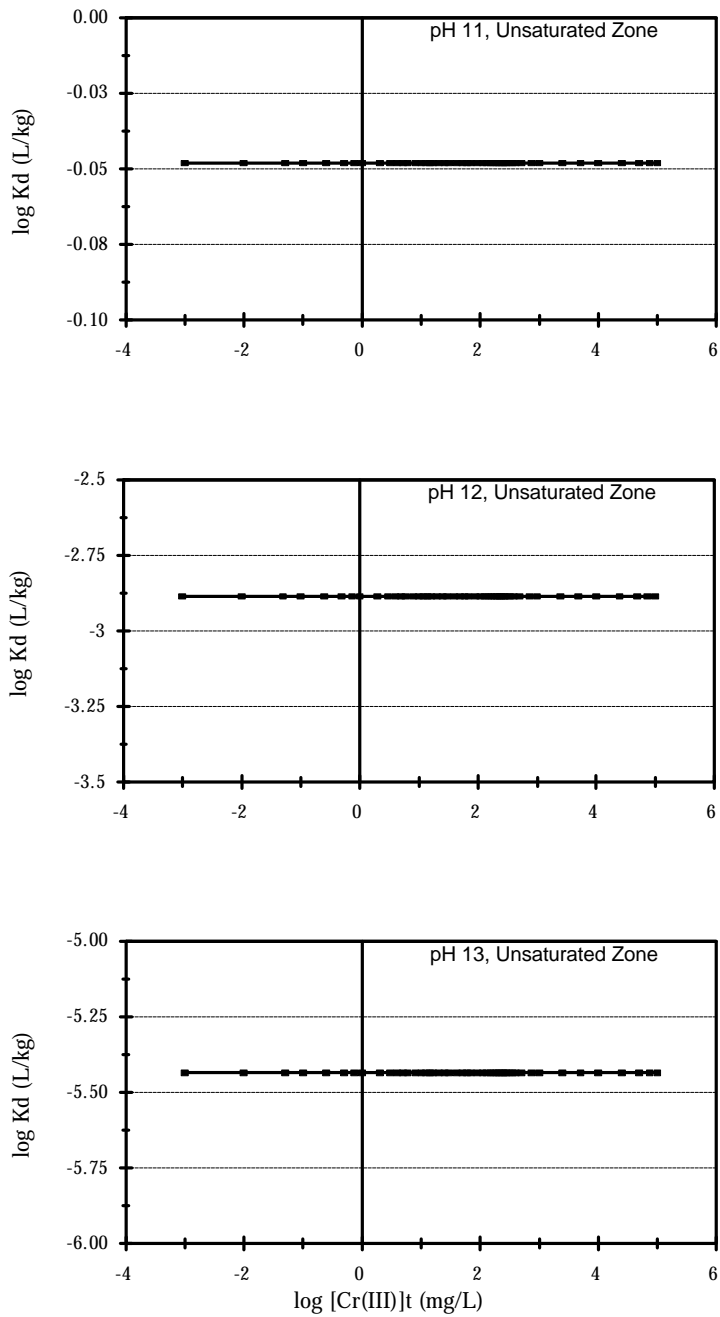


Figure 3.5. Log  $K_d$  (L/kg) vs. log total Cr(III) (mg/L) at pH 11, 12, and 13 in the unsaturated zone.

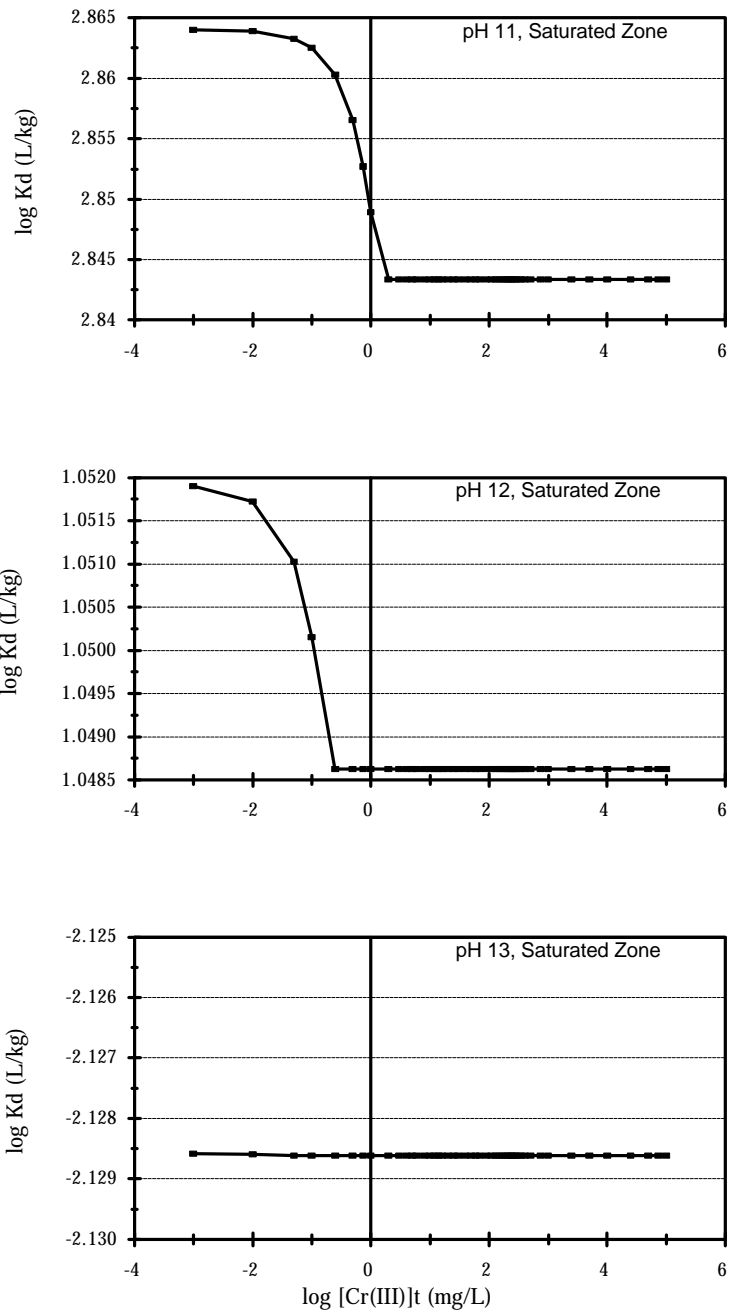


Figure 3.6.  $\log K_d \text{ (L/kg)}$  vs.  $\log \text{ total Cr(III) (mg/L)}$  at pH 11, 12, and 13 in the saturated zone.

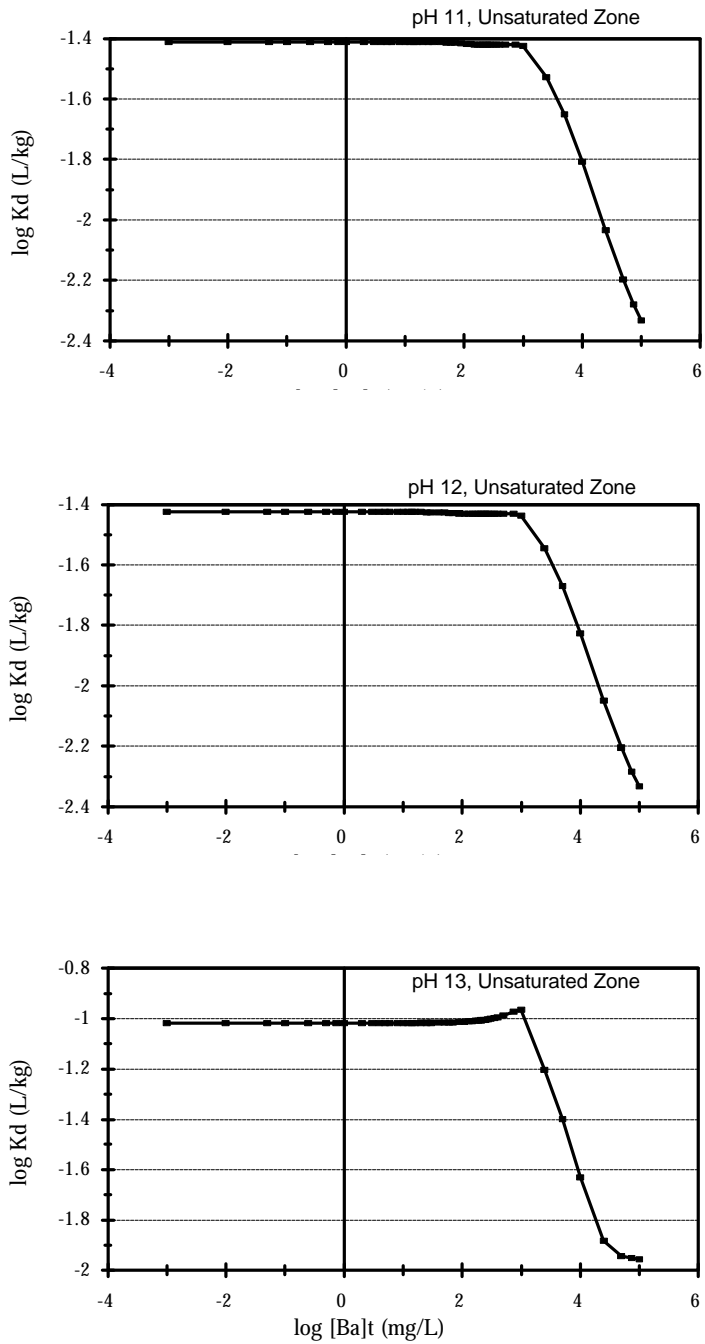


Figure 3.7.  $\log K_d$  (L/kg) vs.  $\log$  total Ba (mg/L) at pH 11, 12, and 13 in the unsaturated zone.

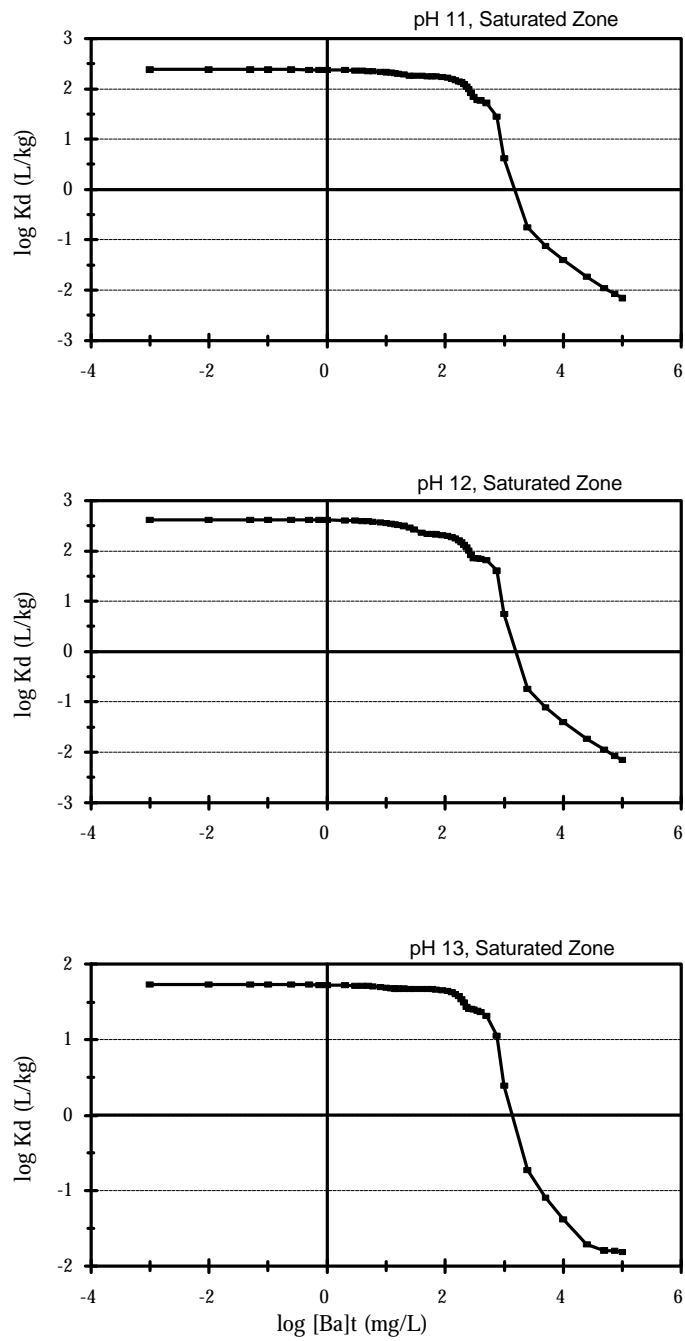


Figure 3.8.  $\log K_d$  (L/kg) vs.  $\log$  total Ba (mg/L) at pH 11, 12, and 13 in the saturated zone.

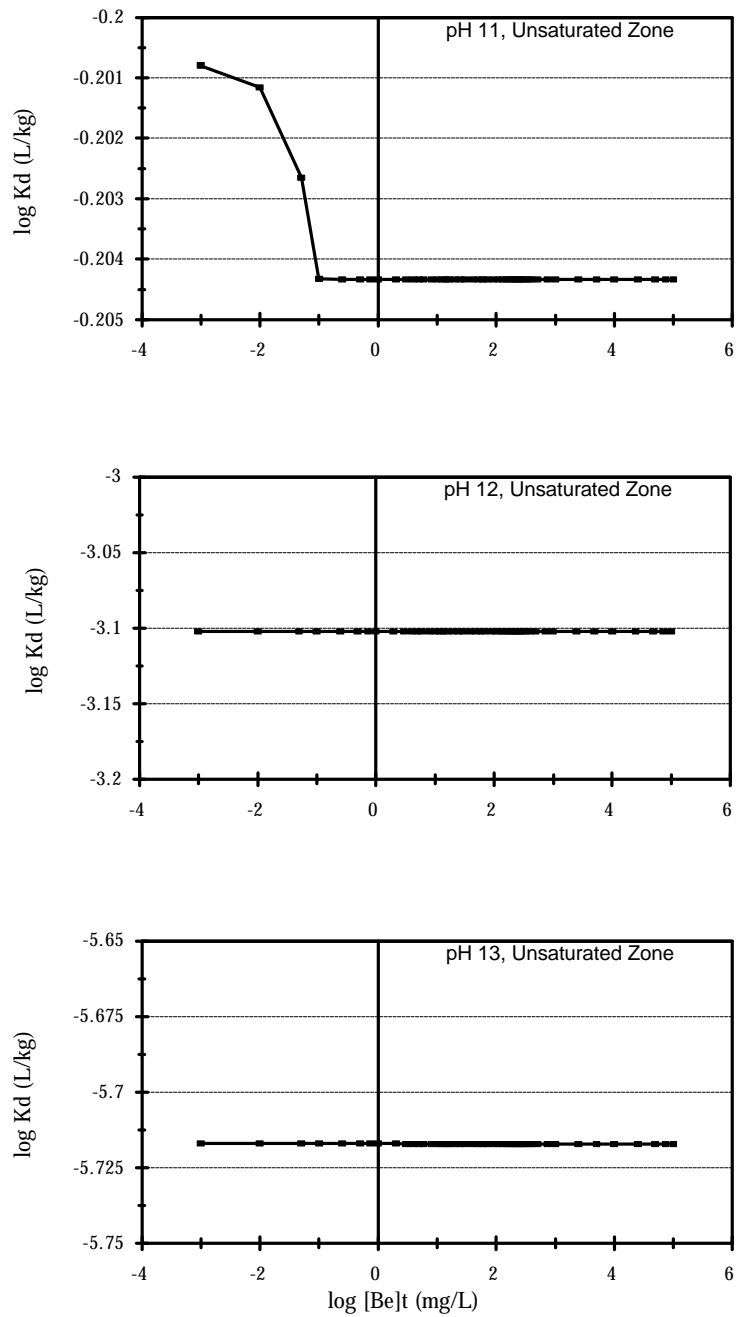


Figure 3.9. Log  $K_d$  (L/kg) vs. log total Be (mg/L) at pH 11, 12, and 13 in the unsaturated zone.

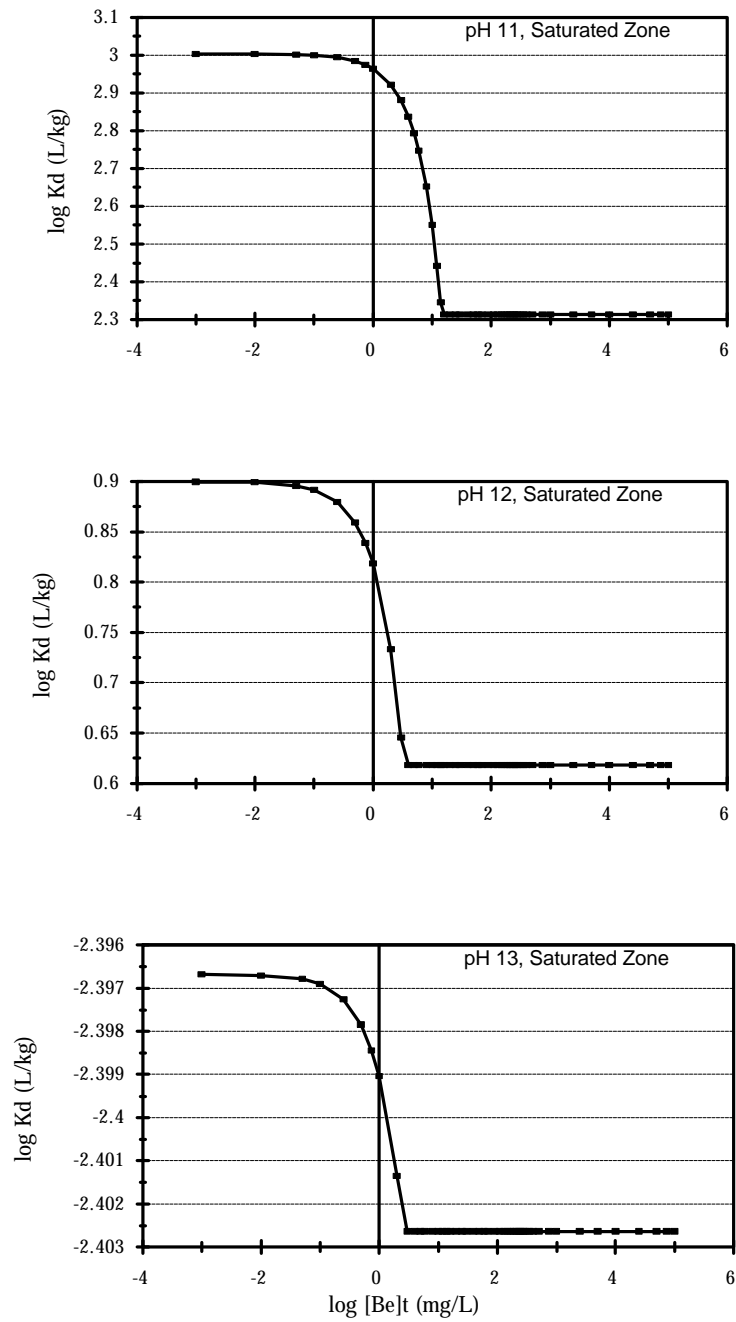


Figure 3.10.  $\log K_d$  (L/kg) vs.  $\log$  total Be (mg/L) at pH 11, 12, and 13 in the saturated zone.

#### 4.0 COMPARISON WITH HWIR RESULTS

An observed trend in previous modeling as well as from the literature is that adsorption of metal cations tends to increase with increasing pH, and adsorption of metal anions tends to decrease. The low pH trend reflects the tendency of sorbed protons to build positive charge on the sorbent surface and thus enhance metal anion adsorption. The high pH trend of enhanced metal cation sorption results from the decreased competition for sorption sites because of the paucity of protons. This study deals with metal cations at high pH. Other factors that effect metal cation adsorption include the concentrations of ligands that complex the metal (in competition with sorption sites), metal cation competition with other specifically adsorbed cations, and changes in ionic strength. (The ionic strength affects the activity coefficients of all species and directly influences the electrostatic potential associated with the HFO surface.) An example of competition from other ligands that is important in this study is formation of aqueous metal hydroxide species. This effect increases with pH, reducing the amount of metal sorbed. As pH increases, the increased tendency for sorption of metal cations due to less competition from protons is offset by the increased affinity of complex formation with hydroxide.

In the current study, an additional complicating factor is the increased concentration of calcium and other major ions from the CKD leachate. Calcium is adsorbed on HFO in accordance with reactions that are similar to those of barium (Dzombak and Morel, 1990). Elevated Ca concentrations tend to reduce the adsorption of other cations. In addition, the increased Na and K concentrations from CKD leachate impact adsorption via their effect on the ionic strength, and increased  $\text{SO}_4$  may complex Ba, Pb, and Cd.

In examining the plots presented in Figures 3.1-3.10, one should note that the saturated zone model conditions correspond much more closely with HWIR modeling than those of the unsaturated zone. This is because of the seven times greater concentration of CKD leachate constituents in the unsaturated zone modeling. Some general observations concerning the plots in Figures 3.1-3.10 are:

- In every case, the unsaturated zone  $K_d$  values are significantly lower than their saturated zone counterparts at the same pH. This is primarily due to the increased competition from the CKD leachate Ca, with some added reduction in sorption due to metal complexing with the added  $\text{SO}_4$ . An additional effect on  $K_d$  may be produced by the impact of the added Na, K, and Cl on the ionic strength, although the direction of change that this would induce is metal-dependent.
- In every case except one, within a particular zone (unsaturated or saturated), the sorption of metal decreases significantly as the pH increases. This is most clearly seen by looking at the progression of results down each page of plots. The one exception is Ba, for which sorption is not much different at pH 12 than for pH 11. At pH 13, Ba sorption is increased slightly in the unsaturated zone and decreased slightly in the saturated zone. This behavior is peculiar to Ba because the Site 1 HFO adsorption reaction for Ba differs

from its counterpart for all the other metals in this study. For all HFO reactions except the Site 1 Ba reaction, the neutral SOH site is deprotonated to  $\text{SO}^-$ , and the metal cation is adsorbed to give SOM (with a +1 charge if M is divalent). For the Site 1 Ba reaction, like its Ca counterpart, the neutral site adsorbs the Ba to give  $\text{SOH}\text{Ba}^{++}$ . Another reason for the “anomalous” behavior of Ba is that it does not have as great a tendency to form aqueous hydroxide species as do the other metals.

- Results that appear as a flat line actually do include the characteristic decrease in  $K_d$  as total metal increases. The flat line appearance occurs when the amount of sorption is so small that variation in it cannot reasonably be calculated or displayed.

The plots on the following pages show the HWIR results corresponding to the highest pH used in HWIR (8.0) and the lowest concentration of leachate organic acids. The concentrations of HFO and natural organic matter were set to medium in the modeling that produced these results. These model conditions were selected to most closely match those of the current study. Results with these conditions are shown for both the unsaturated and saturated zones for the metals Pb, Cd, Cr(III), and Ba. No HWIR results are shown for beryllium because separate modeling was not done for that metal in HWIR. Instead, the  $K_d$  values for barium were used for beryllium as well. As noted above, the saturated zone conditions of the current study (Figures 3.1-3.10) most closely match the HWIR modeling because of the much smaller concentrations of CKD leachate constituents. Comparison of the HWIR plots with the pH 11 saturated zone plots shows the most similar model conditions. In comparing the magnitude of the  $K_d$  values between the pH 11 saturated zone plot and the corresponding HWIR plot, some metals show an increase in the CKD result and some show a decrease. For example, the CKD Pb plots (Figure 3.2) show a general decrease in  $K_d$  with increasing pH. The HWIR plot at pH 8.0 has larger  $K_d$  values than the pH 11 CKD plot, and is thus in keeping with this trend. However, the CKD Cd plots (Figure 3.4) also shows a general decrease with increasing pH, but the HWIR plots at pH 8.0 have smaller  $K_d$  values than the corresponding pH 11 CKD plots. This suggests that for each metal,  $K_d$  increases with pH up to a point, but then begins to fall as pH continues to increase. The pH at which the maximum  $K_d$  is reached varies from one metal to another. Examination of the CKD unsaturated zone results indicates that the pH of maximum  $K_d$  must also depend on the presence or absence of other competitors and complexers in the system. For the current systems, it appears that the  $K_d$  maximum for Pb and Cr(III) occurs at lower pH than for Cd and Ba.



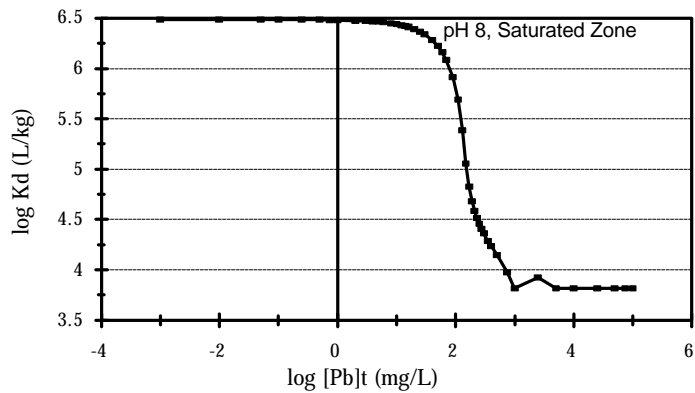
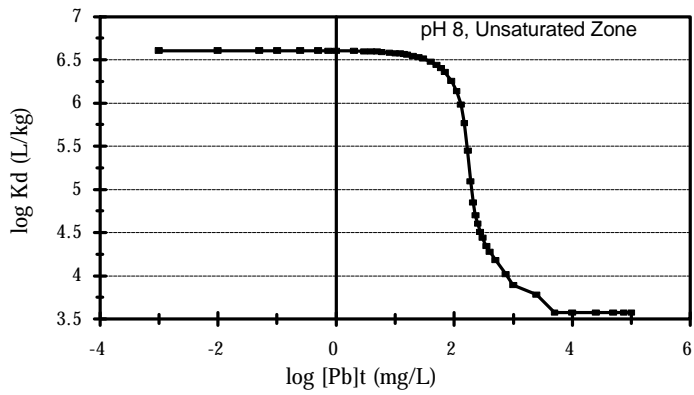


Figure 4.1. HWIR results: log  $K_d$  (L/kg) vs. log total Pb (mg/L) at pH 8 in the unsaturated and saturated zones. Compare with Figures 3.1 and 3.2.

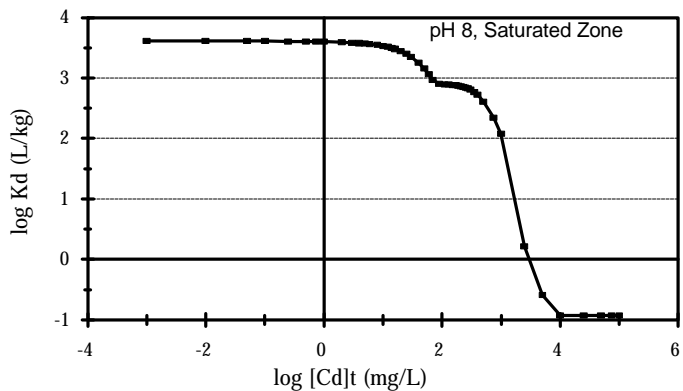
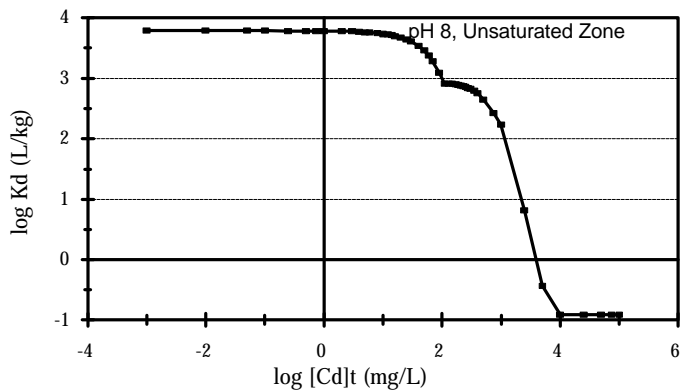


Figure 4.2. HWIR results: log  $K_d$  (L/kg) vs. log total Cd (mg/L) at pH 8 the unsaturated and saturated zones. Compare with Figures 3.3 and 3.4.

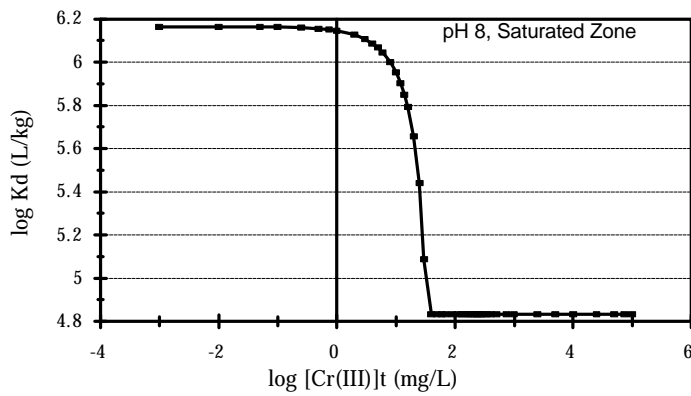
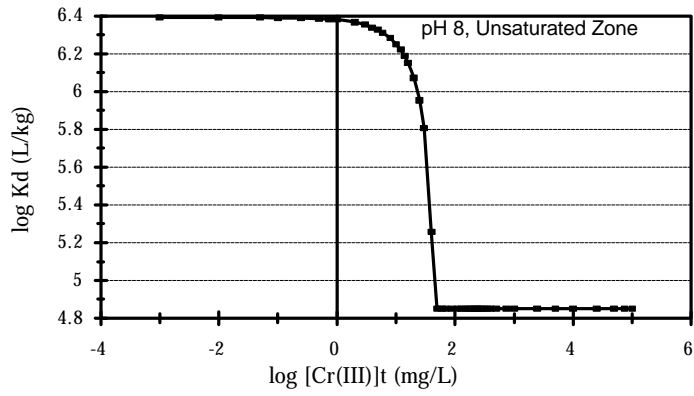


Figure 4.3. HWIR results: log  $K_d$  (L/kg) vs. log total Cr(III) (mg/L) at pH 8 in the unsaturated and saturated zones. Compare with Figures 3.5 and 3.6.

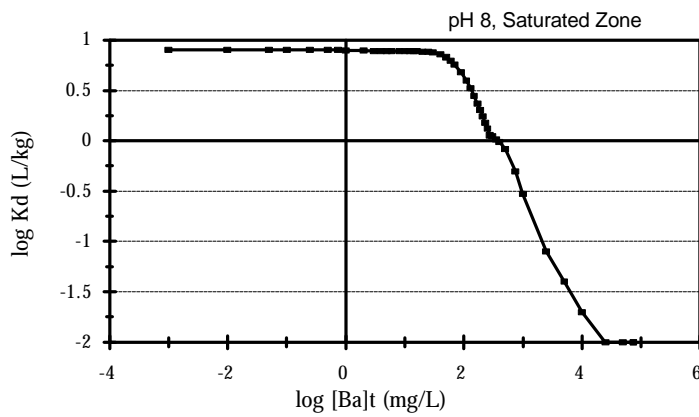
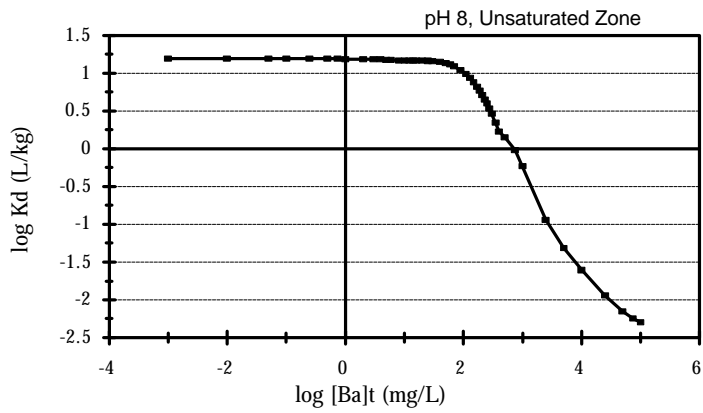


Figure 4.4. HWIR results:  $\log K_d$  (L/kg) vs.  $\log$  total Ba (mg/L) at pH 8 in the unsaturated and saturated zones. Compare with Figures 3.7 and 3.8.

## 5.0 CONCLUSIONS

It appears from the results of this study that several factors influence the  $K_d$  values of Ba, Be, Cd, Cr(III), and Pb at conditions relevant to CKD disposal. The pH and the concentration of inorganic ions in CKD leachate that may compete for adsorption sites are the most important (compare Figures 3.3 and 3.4). It is important to correctly represent the constituents in CKD leachate in order to accurately include these effects in modeling. The current modeling employed concentrations for CKD leachate constituents obtained from a model TCLP simulation on CKD. The most obvious way that this modeling could be improved would be to incorporate real measured concentrations of CKD leachate constituents.

The pH variation in the subsurface due to intrusion of highly alkaline CKD is another area of investigation that should not be ignored. The pH values used here were specified at the outset of the modeling as equilibrium constraints. In the real world, the impact on the ambient groundwater pH will vary with distance from the source. The results presented here indicate that pH is an important variable effecting adsorption of these metals. There is significant variation in  $K_d$  even within the pH range 11 to 13. Another area for improving transport modeling of these metals, although a much more difficult improvement to achieve, is to incorporate variation in pH away from the source in such a way as to allow the model to select the correct  $K_d$  from a matrix that includes values for incremental pH's from 8 to 12 or so.

## 6.0 REFERENCES

- Dzombak, D.A., 1986. Toward a Uniform Model for the Sorption of Inorganic Ions on Hydrated Oxides. Ph.D Thesis. Massachusetts Institute of Technology, Cambridge, MA.
- Dzombak, D.A. and F.M.M. Morel, 1990. Surface Complexation Modeling: Hydrated Ferric Oxide, John Wiley and Sons, New York.
- Haynes, B.W. and G.W. Kramer, 1982. Characterization of U.S. Cement Kiln Dust. U.S. Bureau of Mines, Dept. of the Interior, Information Circular 8885.
- USEPA, 1996. Background Document for Metals. EPA Composite Model for Leachate Migration with Transformation Products (EPACMTP). Volume 1: Methodology. U.S. EPA, Office of Solid Waste, Washington DC, 20460.

Appendix A

Reactions Updated or Added in the MINTEQA2

Thermodynamic Database

The following reactions were updated or added in the thermodynamic database prior to modeling. The source of all solution reactions was *NIST Critical Stability Constants, Reference Database 46, version 2.0*. The source of all HFO reactions was Dzombak and Morel, 1990.

Reaction	Log K	Added(A) or Updated(U)
$\text{Be}^{2+} + \text{H}_2\text{O} - \text{H}^+ = \text{BeOH}^+$	-5.4	A
$\text{Be}^{2+} + 2\text{H}_2\text{O} - 2\text{H}^+ = \text{Be}(\text{OH})_2^{\circ}$	-13.6	A
$\text{Be}^{2+} + 3\text{H}_2\text{O} - 3\text{H}^+ = \text{Be}(\text{OH})_3^-$	-23.2	A
$\text{Be}^{2+} + 4\text{H}_2\text{O} - 4\text{H}^+ = \text{Be}(\text{OH})_4^{2-}$	-37.4	A
$2\text{Be}^{2+} + \text{H}_2\text{O} - \text{H}^+ = \text{Be}_2\text{OH}^{3+}$	-3.18	A
$3\text{Be}^{2+} + 3\text{H}_2\text{O} - 3\text{H}^+ = \text{Be}_3(\text{OH})_3^{3+}$	-8.79	A
$6\text{Be}^{2+} + 8\text{H}_2\text{O} - 8\text{H}^+ = \text{Be}_6(\text{OH})_8^{4+}$	-27.	A
$\text{Be}^{2+} + 2\text{H}_2\text{O} - 2\text{H}^+ = \text{Be}(\text{OH})_2(\text{s},\text{am})$	-7.2	A
$\text{Be}^{2+} + 2\text{H}_2\text{O} - 2\text{H}^+ = \text{Be}(\text{OH})_2(\text{s},\alpha)$	-6.9	A
$\text{Be}^{2+} + 2\text{H}_2\text{O} - 2\text{H}^+ = \text{Be}(\text{OH})_2(\text{s},\beta)$	-6.5	A
$\text{Be}^{2+} + \text{Cl}^- = \text{BeCl}^+$	0.3	A
$\text{Be}^{2+} + \text{SO}_4^{2-} = \text{BeSO}_4^{\circ}$	1.95	A
$\text{Be}^{2+} + \text{CO}_3^{2-} = \text{BeCO}_3^{\circ}$	8.1	A
$\text{Be}^{2+} + \text{Br}^- = \text{BeBr}^+$	0.2	A
$\text{Be}^{2+} + \text{NO}_3^- = \text{BeNO}_3^+$	-0.4	A
$\text{Ba}^{2+} + \text{H}_2\text{O} - \text{H}^+ = \text{BaOH}^+$	-13.36	U

Appendix B

Simulation of the TCLP on Cement Kiln Dust

Using MINTEQA2



The MINTEQA2 simulation of the TCLP on cement kiln dust involves two steps: 1) Specifying the set of components that represent the solid phase including their concentrations, and 2) Specifying the components to represent the leaching solution. For the former, a mineralogical composition of CKD was needed. Haynes and Kramer (1982) provide gross mineralogical compositions for 113 CKD samples collected across the U.S. They express these in terms of weight percent (wt%) calcite, lime, anhydrite, quartz, dolomite, mica, and feldspar. Their wt% values are specified semi-quantitatively as *major*, *minor*, *low* or *very low* with each adjective indicative of a range in wt%. These data were analyzed to establish an average mineralogical composition of CKD as show in the following table.

<b>Mineral</b>	<b>wt%</b>
Calcite	63.2
Lime	15.5
Anhydrite	7.4
Quartz	5.4
Dolomite	3.3
Muscovite	0.5
Orthoclase feldspar	1.3
K <sub>2</sub> SO <sub>4</sub>	1.0
Na <sub>2</sub> SO <sub>4</sub>	1.0
KCl	0.7
NaCl	0.7
<b>TOTAL</b>	<b>100.0</b>

In accordance with the TCLP protocol, the leaching fluid for an alkaline material is 5.7 ml glacial HOAc diluted with water to one liter of solution. The mass of solid to be leached is 1/20 the mass of the leaching solution. This implies a 50 g solid sample for one liter of the leaching solution. The leaching is carried out in a closed zero headspace reactor vessel. This implies no interaction with the atmosphere once the extraction begins. The HOAc solution can be represented in the MINTEQA2 input files as the components H<sup>+</sup> and acetate. The minerals (whose amounts are given by their wt% of the 50 g sample) can be introduced as finite mineral phases or by introducing the corresponding amounts of their components. The temperature was set at 22 °C as specified in the TCLP. After a preliminary run, it was decided that the silicate minerals would be omitted on the basis of geochemical judgement that they would not dissolve in the 18 hour equilibration time of the TCLP experiment. The TCLP simulation input file is

reproduced below. The list of mineral ID numbers (under the heading "4 3" is a guess at equilibrium solids; it helps the model to converge..

```

CKD: Determination of leachate constituents by simulating TCLP
TCLP w/ extraction fluid# 2: 9.958e-2 M HOAc ***FINAL Run***
22.00 MOLAL 0.000 0.00000E+00
0 0 1 1 3 0 0 0 1 1 0 0 0
0 0 0
330 -1.768E-01 -10.00 N /H+1
150 4.900E-01 -2.00 N /Ca+2
460 8.947E-03 -3.00 N /Mg+2
410 1.043E-02 -3.00 N /K+1
500 1.303E-02 -3.00 N /Na+1
732 3.357E-02 -3.00 N /SO4-2
140 3.336E-01 -6.00 N /CO3-2
180 1.068E-02 -3.00 N /Cl-1
992 9.958E-02 -3.00 N /OAc-1

4 3
2003002
5015001
6015001

```

The equilibrium pH of the leachate was 12.47 and the equilibrium ionic strength was 0.18 M. The concentrations of relevant leachate constituents are shown in Table 2.1 (of the main report).

Appendix C

Example MINTEQA2 INPUT FILE

Pb PRODUCTION RUN. UNSAT ZONE, Water Saturation = 77.7%

Md FeO Sorbent, Md Natural Organic Matter

14.00 MG/L 0.000 4.57000E+00

0 0 1 1 3 0 0 0 1 0 2 1 2

TOTAL CONC 600 48

1.000E-02	5.000E-02	1.000E-01	2.500E-01	5.000E-01	7.500E-01
1.000E+00	2.000E+00	3.000E+00	4.000E+00	5.000E+00	6.000E+00
8.000E+00	1.000E+01	1.200E+01	1.400E+01	1.600E+01	2.000E+01
2.500E+01	3.000E+01	4.000E+01	5.000E+01	6.000E+01	7.000E+01
9.000E+01	1.100E+02	1.300E+02	1.500E+02	1.700E+02	1.900E+02
2.100E+02	2.300E+02	2.500E+02	2.750E+02	3.000E+02	3.500E+02
4.000E+02	5.000E+02	7.500E+02	1.000E+03	2.500E+03	5.000E+03
1.000E+04	2.500E+04	5.000E+04	7.500E+04	1.000E+05	

PbMM1lux.PRN 600

4 1 7

1.525E+01 600.00 0.000 0.000 81

999	9.400E+01	-2.00	n	/Charge-
330	0.000E+00	-8.00	y	/H+1
600	1.000E-03	-6.24	y	/
30	2.000E-01	-5.13	y	/Al+3
150	2.883E+03	-2.92	y	/Ca+2
281	2.000E-01	-5.45	y	/Fe+3
460	1.400E+01	-3.24	y	/Mg+2
470	4.000E-02	-6.14	y	/Mn+2
410	4.109E+02	-4.13	y	/K+1
500	3.220E+02	-3.02	y	/Na+1
140	1.870E+02	-2.51	y	/CO3-2
130	3.000E-01	-5.43	y	/Br-1
180	3.940E+02	-3.37	y	/Cl-1
492	1.000E+00	-4.79	y	/NO3-1
580	9.000E-02	-6.02	y	/PO4-3
732	6.570E+02	-3.58	y	/SO4-2
145	2.439E-05	-6.50		/
146	5.758E-03	-6.17		/
811	8.568E-04	-4.45	y	/ADS1TYP1
812	3.427E-02	-2.84	y	/ADS1TYP2
813	0.000E+00	0.00	y	/ADS1PSIo

3 1

330 11.0000 0.0000 /H+1

6 4

813 0.0000 0.0000 /ADS1PSIo

3046001

2003002

0.0000 0.0000 /

3028100

0.0000 0.0000 /

2 25

8113301	=SO1-	0.0000	-8.9300	0.000	0.000	-1.00	0.00	0.00	0.0000
0.00	3	1.000	811	-1.000	330	-1.000	813	0.000	0
0.000	0	0.000	0	0.000	0	0.000	0	0.000	0
0	0.000	0	0.000	0	0.000	0	0.000	0	0.000
8113302	=SO1H2+	0.0000	7.2900	0.000	0.000	1.00	0.00	0.00	0.0000
0.00	3	1.000	811	1.000	330	1.000	813	0.000	0
0.000	0	0.000	0	0.000	0	0.000	0	0.000	0
0	0.000	0	0.000	0	0.000	0	0.000	0	0.000
8123301	=SO2-	0.0000	-8.9300	0.000	0.000	-1.00	0.00	0.00	0.0000
0.00	3	1.000	812	-1.000	330	-1.000	813	0.000	0
0.000	0	0.000	0	0.000	0	0.000	0	0.000	0
0	0.000	0	0.000	0	0.000	0	0.000	0	0.000
8123302	=SO2H2+	0.0000	7.2900	0.000	0.000	1.00	0.00	0.00	0.0000
0.00	3	1.000	812	1.000	330	1.000	813	0.000	0
0.000	0	0.000	0	0.000	0	0.000	0	0.000	0
0	0.000	0	0.000	0	0.000	0	0.000	0	0.000
8112110	=SO1CrOH+	0.0000	11.5600	0.000	0.000	1.00	0.00	0.00	0.0000

0.00 4	1.000 811	1.000 211	1.000 813	-1.000 2	0.000 0	0.000 0	0.000 0
0.000 0	0.000 0	0.000 0	0.000 0	0.000 0	0.000 0	0.000 0	0.000 0
0 0.000	0 0.000	0 0.000	0	0	0	0	0
8116000	=SO1Pb+	0.0000	4.6500	0.000 0.000	1.00 0.00	0.00 0.0000	0.0000
0.00 5	1.000 811	-1.000 330	1.000 813	1.000 600	1.000 2	0.000 0	0
0.000 0	0.000 0	0.000 0	0.000 0	0.000 0	0.000 0	0.000 0	0
0 0.000	0 0.000	0 0.000	0	0	0	0	0
8126000	=SO2Pb+	0.0000	0.3000	0.000 0.000	1.00 0.00	0.00 0.0000	0.0000
0.00 5	1.000 812	-1.000 330	1.000 813	1.000 600	1.000 2	0.000 0	0
0.000 0	0.000 0	0.000 0	0.000 0	0.000 0	0.000 0	0.000 0	0
0 0.000	0 0.000	0 0.000	0	0	0	0	0
8111600	=SO1Cd+	0.0000	0.4700	0.000 0.000	1.00 0.00	0.00 0.0000	0.0000
0.00 5	1.000 811	-1.000 330	1.000 813	1.000 160	1.000 2	0.000 0	0
0.000 0	0.000 0	0.000 0	0.000 0	0.000 0	0.000 0	0.000 0	0
0 0.000	0 0.000	0 0.000	0	0	0	0	0
8121600	=SO2Cd+	0.0000	-2.9000	0.000 0.000	1.00 0.00	0.00 0.0000	0.0000
0.00 5	1.000 812	-1.000 330	1.000 813	1.000 160	1.000 2	0.000 0	0
0.000 0	0.000 0	0.000 0	0.000 0	0.000 0	0.000 0	0.000 0	0
0 0.000	0 0.000	0 0.000	0	0	0	0	0
8111100	=SO1Be+	0.0000	5.7000	0.000 0.000	1.00 0.00	0.00 0.0000	0.0000
0.00 5	1.000 811	-1.000 330	1.000 813	1.000 110	1.000 2	0.000 0	0
0.000 0	0.000 0	0.000 0	0.000 0	0.000 0	0.000 0	0.000 0	0
0 0.000	0 0.000	0 0.000	0	0	0	0	0
8121100	=SO2Be+	0.0000	3.3000	0.000 0.000	1.00 0.00	0.00 0.0000	0.0000
0.00 5	1.000 812	-1.000 330	1.000 813	1.000 110	1.000 2	0.000 0	0
0.000 0	0.000 0	0.000 0	0.000 0	0.000 0	0.000 0	0.000 0	0
0 0.000	0 0.000	0 0.000	0	0	0	0	0
8111000	=SO1HBa++	0.0000	5.4600	0.000 0.000	2.00 0.00	0.00 0.0000	0.0000
0.00 3	1.000 811	1.000 100	2.000 813	0.000 0	0.000 0	0.000 0	0
0.000 0	0.000 0	0.000 0	0.000 0	0.000 0	0.000 0	0.000 0	0
0 0.000	0 0.000	0 0.000	0	0	0	0	0
8121000	=SO2Ba+	0.0000	-7.2000	0.000 0.000	1.00 0.00	0.00 0.0000	0.0000
0.00 4	1.000 812	-1.000 330	1.000 813	1.000 100	0.000 0	0.000 0	0
0.000 0	0.000 0	0.000 0	0.000 0	0.000 0	0.000 0	0.000 0	0
0 0.000	0 0.000	0 0.000	0	0	0	0	0
8111500	=SO1HCa++	0.0000	4.9700	0.000 0.000	2.00 0.00	0.00 0.0000	0.0000
0.00 3	1.000 811	1.000 150	2.000 813	0.000 0	0.000 0	0.000 0	0
0.000 0	0.000 0	0.000 0	0.000 0	0.000 0	0.000 0	0.000 0	0
0 0.000	0 0.000	0 0.000	0	0	0	0	0
8121500	=SO2Ca+	0.0000	-5.8500	0.000 0.000	1.00 0.00	0.00 0.0000	0.0000
0.00 4	1.000 812	-1.000 330	1.000 813	1.000 150	0.000 0	0.000 0	0
0.000 0	0.000 0	0.000 0	0.000 0	0.000 0	0.000 0	0.000 0	0
0 0.000	0 0.000	0 0.000	0	0	0	0	0
8117320	=S1SO4-	0.0000	7.7800	0.000 0.000	-1.00 0.00	0.00 0.0000	0.0000
0.00 5	1.000 811	1.000 330	-1.000 813	1.000 732	-1.000 2	0.000 0	0
0.000 0	0.000 0	0.000 0	0.000 0	0.000 0	0.000 0	0.000 0	0
0 0.000	0 0.000	0 0.000	0	0	0	0	0
8127320	=S2SO4-	0.0000	7.7800	0.000 0.000	-1.00 0.00	0.00 0.0000	0.0000
0.00 5	1.000 812	1.000 330	-1.000 813	1.000 732	-1.000 2	0.000 0	0
0.000 0	0.000 0	0.000 0	0.000 0	0.000 0	0.000 0	0.000 0	0
0 0.000	0 0.000	0 0.000	0	0	0	0	0
8117321	=SO1HSO4-2	0.0000	0.7900	0.000 0.000	-2.00 0.00	0.00 0.0000	0.0000
0.00 3	1.000 811	-2.000 813	1.000 732	0.000 0	0.000 0	0.000 0	0
0.000 0	0.000 0	0.000 0	0.000 0	0.000 0	0.000 0	0.000 0	0
0 0.000	0 0.000	0 0.000	0	0	0	0	0
8127321	=SO2HSO4-2	0.0000	0.7900	0.000 0.000	-2.00 0.00	0.00 0.0000	0.0000
0.00 3	1.000 812	-2.000 813	1.000 732	0.000 0	0.000 0	0.000 0	0
0.000 0	0.000 0	0.000 0	0.000 0	0.000 0	0.000 0	0.000 0	0
0 0.000	0 0.000	0 0.000	0	0	0	0	0
8115800	=S1H2PO4	0.0000	31.2900	0.000 0.000	0.00 0.00	0.00 0.0000	0.0000
0.00 4	1.000 811	1.000 580	3.000 330	-1.000 2	0.000 0	0.000 0	0
0.000 0	0.000 0	0.000 0	0.000 0	0.000 0	0.000 0	0.000 0	0
0 0.000	0 0.000	0 0.000	0	0	0	0	0
8125800	=S2H2PO4	0.0000	31.2900	0.000 0.000	0.00 0.00	0.00 0.0000	0.0000

```

0.00 4    1.000 812    1.000 580    3.000 330   -1.000  2    0.000  0    0.000  0
0.000  0    0.000  0    0.000  0    0.000  0    0.000  0    0.000  0
0 0.000  0    0.000  0    0.000  0
8115801 =S1HPO4-    0.0000    25.3900    0.000    0.000-1.00 0.00 0.00    0.0000
0.00 5    1.000 811   -1.000 813    1.000 580    2.000 330   -1.000  2    0.000  0
0.000  0    0.000  0    0.000  0    0.000  0    0.000  0    0.000  0
0 0.000  0    0.000  0    0.000  0
8125801 =S2HPO4-    0.0000    25.3900    0.000    0.000-1.00 0.00 0.00    0.0000
0.00 5    1.000 812   -1.000 813    1.000 580    2.000 330   -1.000  2    0.000  0
0.000  0    0.000  0    0.000  0    0.000  0    0.000  0    0.000  0
0 0.000  0    0.000  0    0.000  0
8115802 =S1PO4-2    0.0000    17.7200    0.000    0.000-2.00 0.00 0.00    0.0000
0.00 5    1.000 811    1.000 580    1.000 330   -2.000 813   -1.000  2    0.000  0
0.000  0    0.000  0    0.000  0    0.000  0    0.000  0    0.000  0
0 0.000  0    0.000  0    0.000  0
8125802 =S2PO4-2    0.0000    17.7200    0.000    0.000-2.00 0.00 0.00    0.0000
0.00 5    1.000 812    1.000 580    1.000 330   -2.000 813   -1.000  2    0.000  0
0.000  0    0.000  0    0.000  0    0.000  0    0.000  0    0.000  0
0 0.000  0    0.000  0    0.000  0

```